

**Polyphased inversions of an intracontinental rift: case study of the Marrakech High Atlas, Morocco**

R. Leprêtre<sup>1,2</sup>, Y. Missenard<sup>1</sup>, J. Barbarand<sup>1</sup>, C. Gautheron<sup>1</sup>, I. Juvie<sup>1,3</sup>, O. Saddiqi<sup>4</sup>

<sup>1</sup>GEOPS, Univ Paris Sud, CNRS, Université Paris-Saclay, Rue du Belvédère, Bât. 504, Orsay, F-91405, France

<sup>2</sup>Département Géosciences et Environnement, Univ. Cergy-Pontoise, Site de Neuville/Oise, F-95000 Cergy-Pontoise, France

<sup>3</sup>IGE, Université Joseph Fourier, CS 40700, 38058, Grenoble, France

<sup>4</sup>Université Hassan II, Faculté des Sciences, Casablanca, Morocco

**Contents of this file**

Text S1 to S4  
Figures S1 to S9  
Tables S1 to S3

**Introduction**

This supporting information provides further details on the numerous modeling experiments presented in the main text.

**Text S1.** Detailed methodology for thermal modeling of the different samples using QTQt.

The thermal modeling, using QTQt (Gallagher, 2012) was tuned with the He-trapping/diffusion model of Flowers et al. (2009). The fission track kinetics parameter is the updated one found in Ketcham et al. (2007). In the course of the modeling, QTQt was tuned with 200, 000 iterations : 100, 000 for the burn-in phase and 100, 000 for the post-burn-in phase.

The forward modeling for the different samples described in the Text S2-4 were led with HeFTy (Ketcham et al., 2005) to model the AHe ages with the Flowers et al. (2009) model.

**Text S2.** Thermal modeling of combined samples AZ01-02 and AZ03-04.

Samples AZ03 and AZ04, AZ01 and AZ02 were two sets of samples from the same pluton massif in Azegour (Figure 2a). They were taken for each couple at the same elevation, and between the two datasets exists a c.a. 350 meters drop in elevation (Table SD1). For each couple, only one AFT age was produced: for AZ03 (elevation 1820 m;  $131 \pm 8$  Ma) and for AZ02 (elevation 1480 m;  $136 \pm 9$  Ma). Anyway, a singular AHe dataset was produced for each sample. We thus joined the AHe datasets in only one for each couple of samples and used the single AFT dataset of one of them to combine AZ03 and AZ04, AZ01 and AZ02 in two combined samples AZ01-02 and AZ03-04.

Furthermore, we modeled these two samples with the same stratigraphical constraints taking into account the difference in elevation, in terms of temperature difference ( $\sim 10^\circ\text{C}$  with a classical  $30^\circ\text{C.km}^{-1}$  geotherm). The main stratigraphical constraints used for the inverse modeling were the following for the uppermost sample AZ03-04, corrected for the drop in elevation for AZ01-02: (1) samples were at the surface by the beginning of Middle Jurassic; (2) the extended Middle Jurassic to Cenomanian-Turonian cover (c.a. 400 to 700 meter- thick); (3) samples were consequently at depths of c.a. 400-700 meters at the onset of Eocene times.

From this basis, we led the inverse modeling with time-temperature boxes with varying sizes. Three tests were done, whose results are presented in Figure S6 and Table S2. For the final choice, we selected the inverse modeling presenting the best LL values for both combined samples (scenario HT3), which is the thermal model given in Figure 7b).

**Text S3.** Thermal modeling of sample BO01 (Figure S7)

BO01 sample is located in the northernmost part of the WB1 block (Figure 2a). Since its position with respect to the NAF is not clear, we decided to put no Mesozoic-Cenozoic constraint within the inverse modeling. We only used a (T,t) box between 400-300 Ma and 0-

140 °C to make the thermal path begin in the Paleozoic since the AFT age is quite old and may include fission tracks generated early in the thermal history of the sample.

**Text S4.** Thermal modeling of combined sample ALM01-02 and sample AD01

In the WB2 block, in the same way as for the AZ01-04 samples, we used a combined sample with ALM01 and ALM02 sample. No stratigraphical constraints could be used in this block where no Mesozoic-Cenozoic sedimentary remnants are preserved. A prior test was led with inverse modeling for both samples AD01 and ALM01-02 (Figure S8). The combined sample ALM01-02 gave good predictions whereas the AD01 sample did not yield stable solutions with QTQt.

Samples ALM01 and ALM02 are located 900 meters higher than AD01 in the same block WB2. Thus, we used forward modeling mimicking the thermal history of combined sample ALM01-02 with the elevation drop converted into temperature ( $\sim 27$  °C with a classical  $30^{\circ}\text{C.km}^{-1}$ ). We tested eight different thermal paths with forward modeling, whose results are presented in Table S3 and in Figure S9.

**Figure S1.** Track lengths distributions for the wMHA and new length datasets for samples of Missenard et al. [2008] samples. Readers are invited to check the works of Ghorbal [2009] and F. El Haimer [2014] for others length datasets, only summarized in the tables of the main manuscript text.

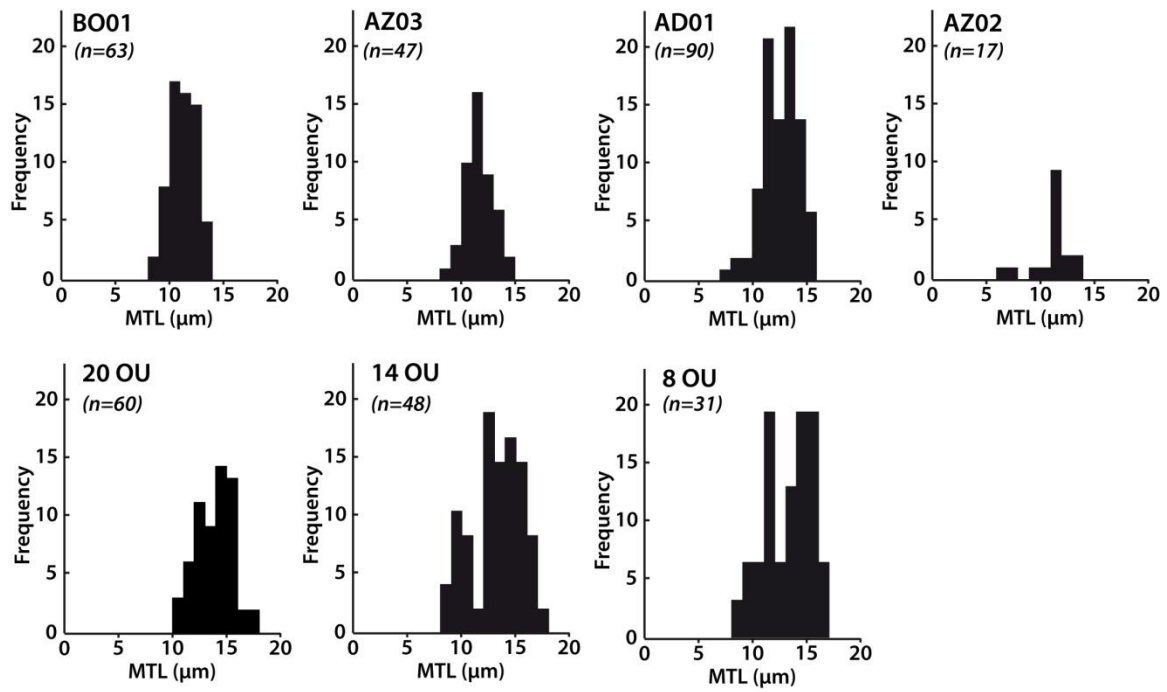


**Figure S2.** AHe ages versus the eU content plots, for the northern and southern forelands of the cMHA cross-section (Figures 2b, 3b-c). (a) AHe age-eU plot for the northern foreland (Block NF). The AFT ages of samples NS0401 and NS0404 are indicated by a horizontal light grey bar. Dashed arrows indicate the putative relationship between AHe ages and the eU content for each “valid” sample. NS0403 sample is excluded since replicates show a strong internal variation in their Th/U ratio. NS0401-02 samples are treated together since they come from the same initial sample [Ghorbal, 2009]. (b-e) AHe age-eU plots for the southern foreland (Blocks SF1 to SF3).

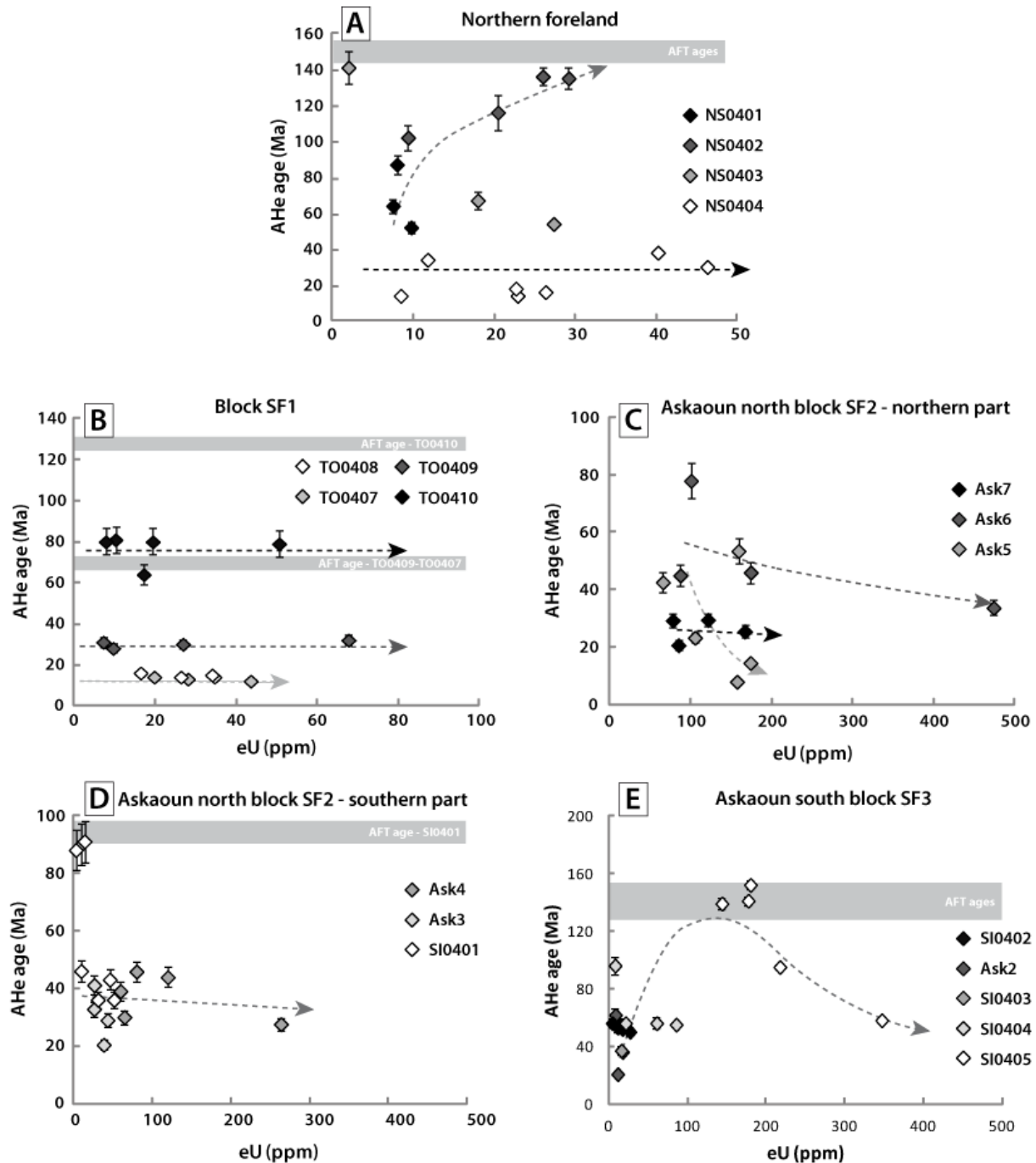


**Figure S3.** AHe ages versus the eU content plots, for the wMHA cross-section (Figures 2a, 3b-c). (a-c) AHe-eU plot for samples from the different groups of samples. For each plot, the dashed colored line behind the datapoints sketches the putative relationship between the single-grain AHe ages and the eU content.

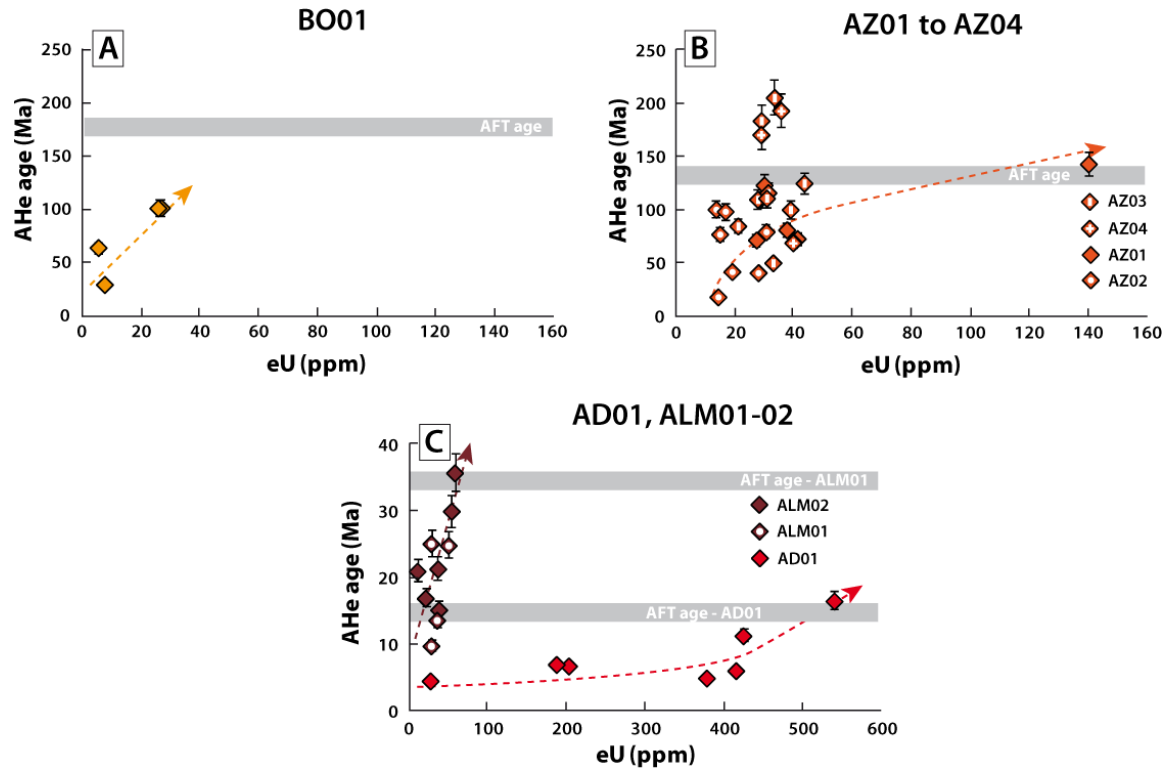


**Figure S4.** Thermal modeling tests for the northern foreland NS0401-02 samples.

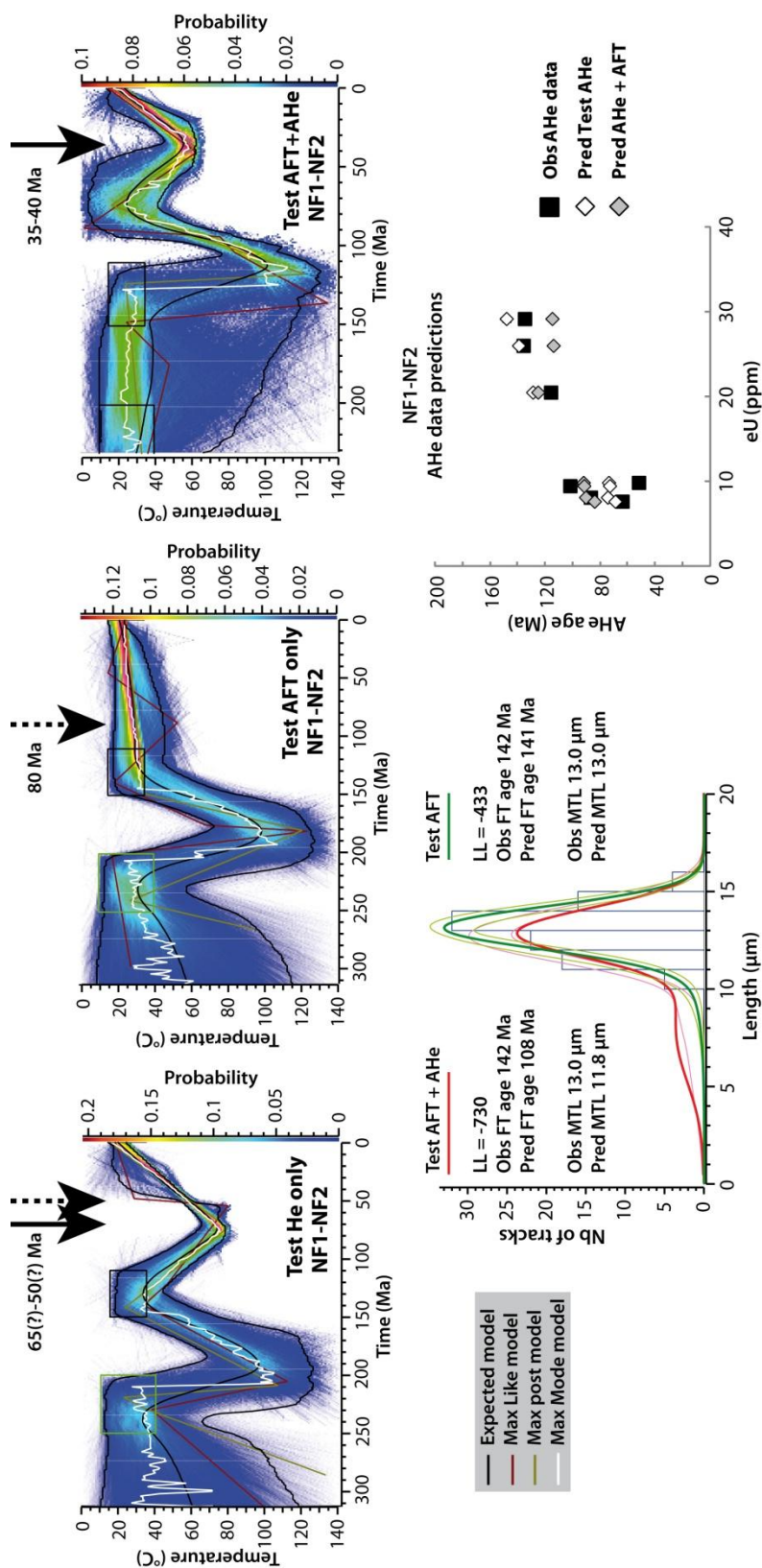


**Figure S5.** Thermal modeling tests for the northern foreland NS0404 sample.

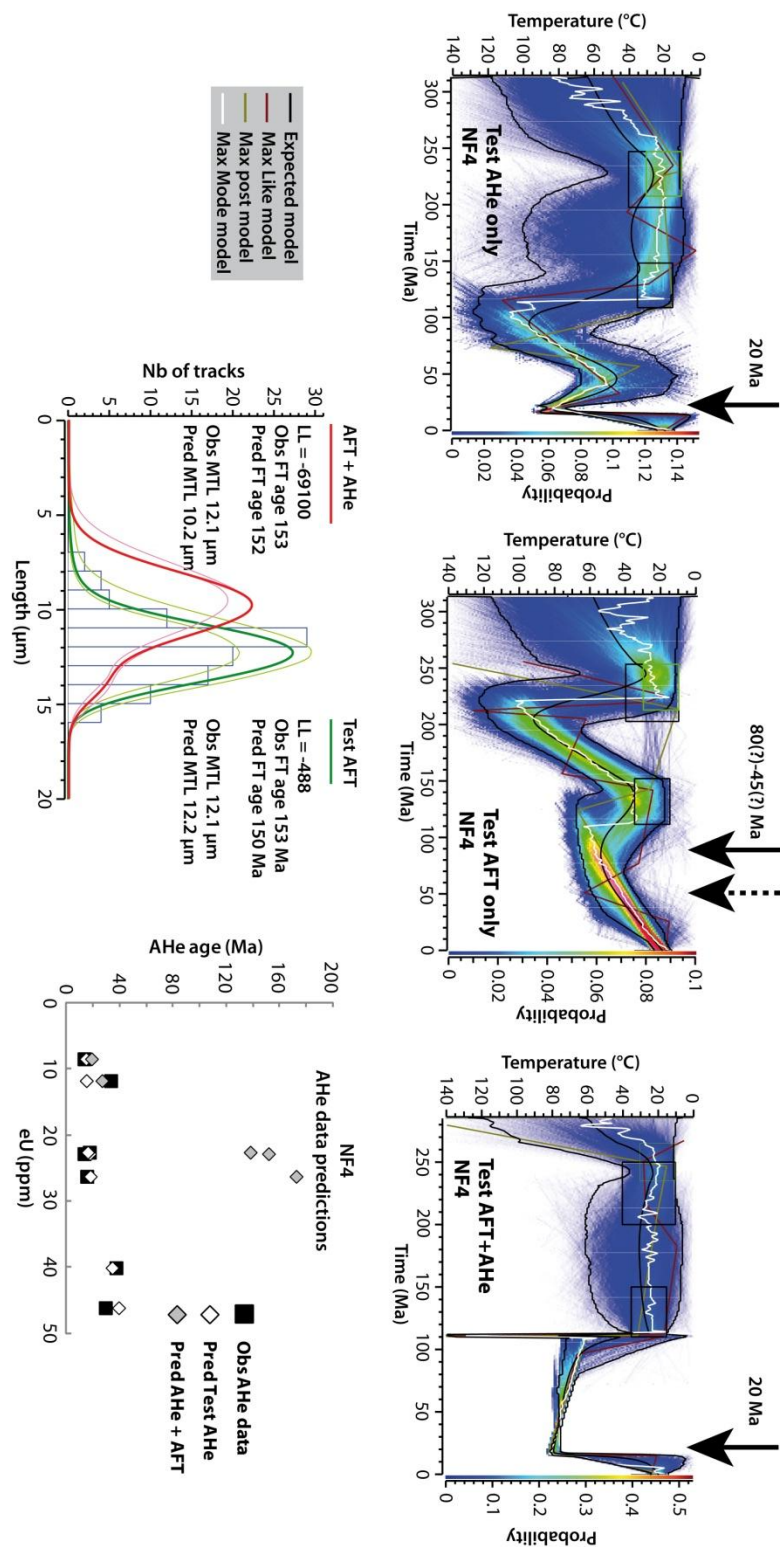




**Figure S6.** Thermal modeling of samples AZ01-AZ04 in block WB1.

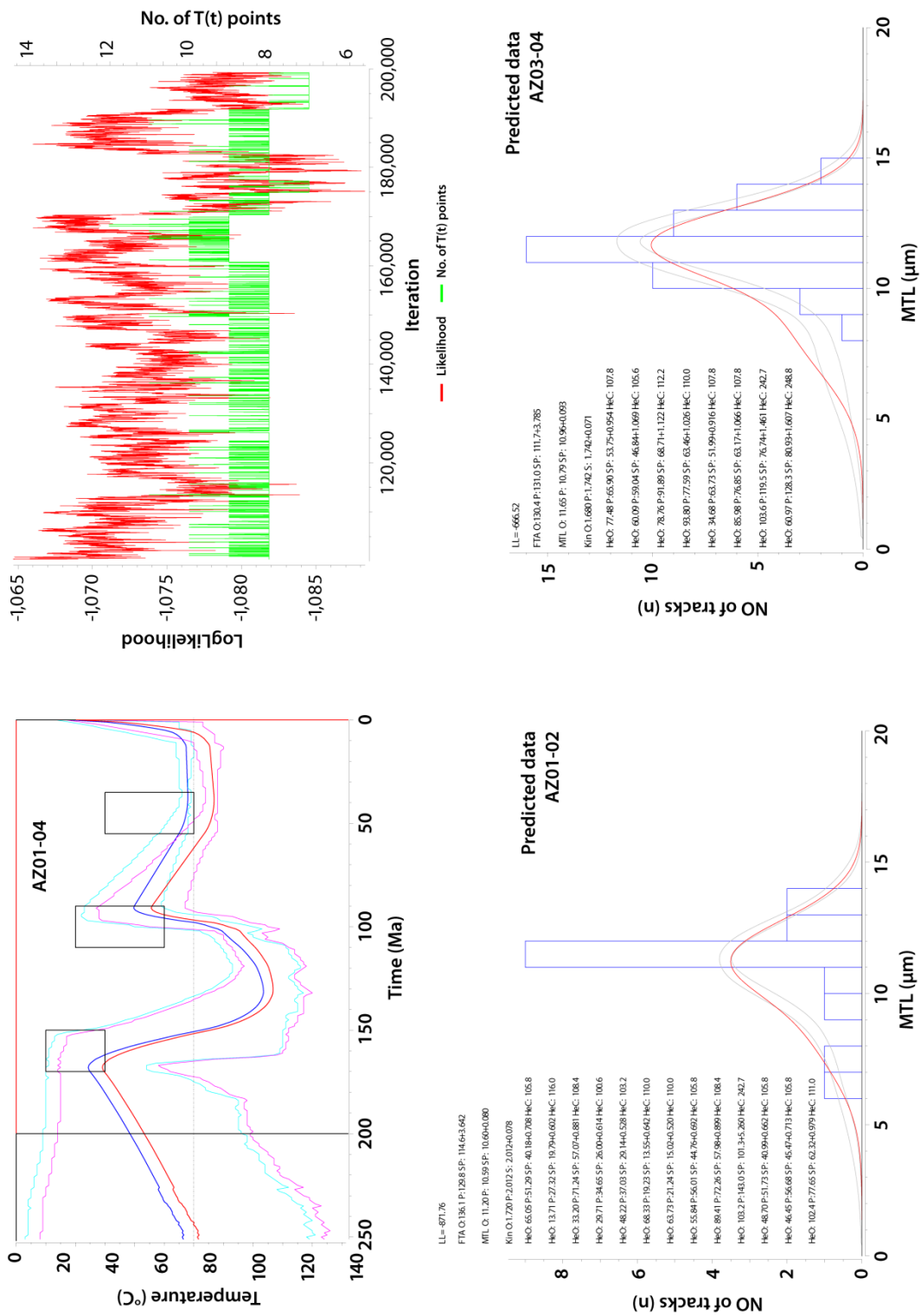


**Figure S7.** Thermal modeling of BO01 sample.

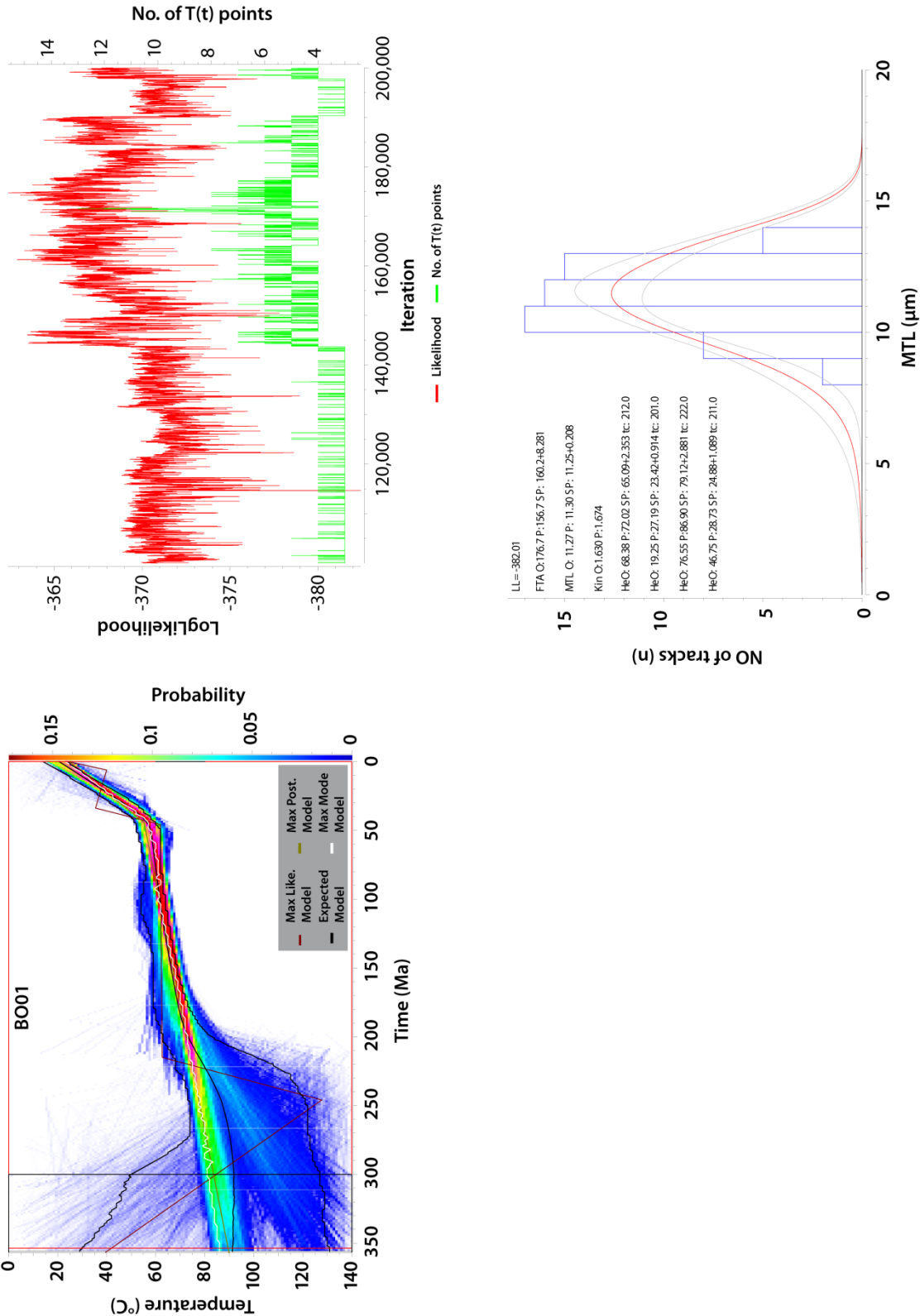
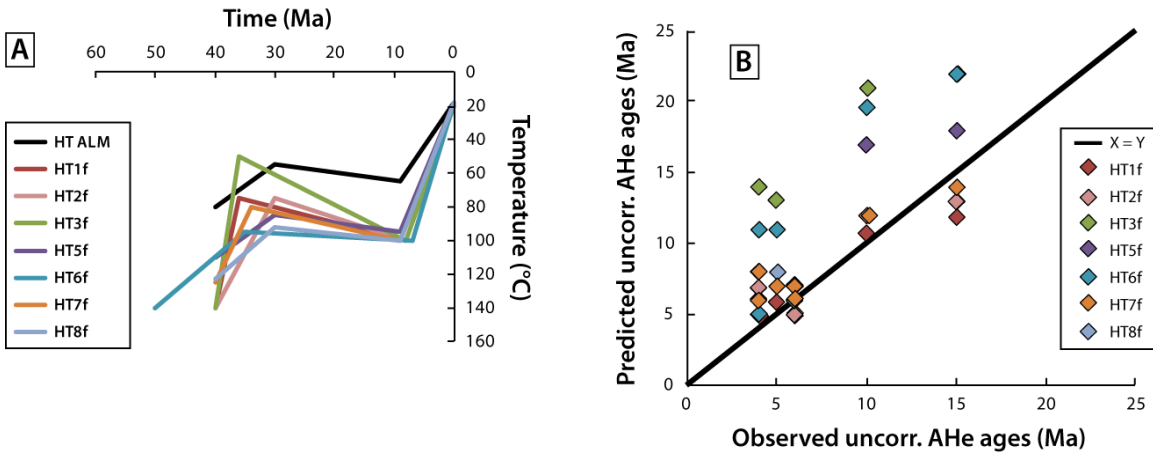


Figure 1 consists of three panels. The top panel is a 2D histogram showing the distribution of Temperature (°C) on the y-axis (ranging from 20 to 140) versus Time (Ma) on the x-axis (ranging from 0 to 60). The histogram is color-coded by density, with a legend indicating 'Max Like.', 'Model', 'Expected', and 'Max Mode'. The middle panel is a line plot of Loglikelihood (y-axis, ranging from -194 to -184) versus Iteration (x-axis, ranging from 0 to 200,000). It shows two data series: 'Likelihood' (red line) and 'No. of T(t) points' (green line). The bottom panel is a line plot of 'No of tracks (n)' (y-axis, ranging from 0 to 25) versus 'MTL (μm)' (x-axis, ranging from 0 to 20). It displays a red curve representing the distribution of tracks across different MTL values.

**Figure S9.** Forward modeling for sample AD01.



**Table S1.** Location and elevation of the samples.

	Sample	Rock-type	Location	Elevation (m)
<b>Central MHA</b>				
<i>Northern Foreland</i>	<b>NS0401</b>	<b>metapelite</b>	31°18'55.00"N	1029
			7°57'50.00"W	
	<b>NS0402</b>	<b>metapelite</b>	31°18'55.00"N	1029
			7°57'50.00"W	
	<b>NS0403</b>	<b>metapelite</b>	31°17'31.00"N	1067
			7°57'53.00"W	
	<b>NS0404</b>	<b>sandstone</b>	31°13'34.00"N	1278
			7°58'34.00"W	
<i>Inner belt</i>	<b>08OU</b>	volcanodet.	31°17'2.73"N	1100
			7°42'4.20"W	
	<b>05OU</b>	gneiss	31°16'53.82"N	1230
			7°41'52.58"W	
	<b>OU0507</b>	eyed-gneiss	31°11'54"N	1338
			06°51'30"W	
	<b>13OU</b>	gneiss	31°14'54.01"N	1265
			7°40'9.60"W	
	<b>01OU</b>	gneiss	31°14'54.01"N	1360
			7°40'9.60"W	
	<b>TO0401</b>	granite	31° 7'37.00"N	1941
			7°55'11.00"W	
	<b>TO0402</b>	granite	31° 6'52.00"N	2291
			7°55'11.00"W	
	<b>17OU</b>	granodio	31°14'18.33"N	1480

		7°39'37.81"W	
<b>OU0506</b>	eyed-gneiss	31°13'03"N	1795
		06°52'42"W	
<b>15OU</b>	granodiorite	31°13'2.56"N	1580
		7°41'37.22"W	
<b>14OU</b>	eyed-gneiss	31°13'2.56"N	1560
		7°41'37.22"W	
<b>20OU</b>	amphibolt	31°13'2.56"N	1520
		7°41'37.22"W	
<b>TO0403</b>	rhyolite	31° 5'34.00"N	2544
		7°54'56.00"W	
<b>TO0404</b>	rhyolite	31° 5'10.00"N	2937
		7°55'50.00"W	
<b>OU0505</b>	granite	31°14'01"N	2549
		07°39'49"W	
<b>OU0504</b>	granite	31°15'06"N	2722
		07°48'38"W	
<b>OU0503</b>	granite	31°11'23"N	2883
		07°50'46"W	
<b>OU0502</b>	granite	31°10'17"N	3000
		07°50'57"W	
<b>OU0501</b>	granite	31°12'20.56"N	3150
		7°38'30.53"W	
<b>TO0405</b>	granite	31° 1'37.00"N	2500
		7°52'54.00"W	
<b>2SA</b>	volcanodet.	31° 5'42.10"N	2150
		7°40'37.90"W	
<b>1SA</b>	volcanodet.	31° 1'10.82"N	1900
		7°50'25.86"W	

	<b>TO0406</b>	granite	31° 0'46.04"N 7°48'37.65"W	1934
	<i>SAF</i>		<i>SAF</i>	
<i>Southern Foreland Block SF1</i>	<b>01Si</b>	volcanodet.	31° 3'24.19"N 7°41'3.30"W	2100
	<b>TO0408</b>	granite	30°57'7.00"N 7°53'31.00"W	1555
	<b>TO0407</b>	granite	30°58'25.00"N 7°49'19.00"W	1686
	<b>T00409</b>	granite	30°52'23.00"N 7°53'31.00"W	1333
	<b>02Si</b>	granite	30°53'12.72"N 7°51'19.68"W	1340
	<b>T00410</b>	granite	30°45'31.00"N 7°55'23.00"W	1088
<i>Southern Foreland Block SF2</i>	<b>Ask7</b>	granite	30°53'52.80"N 7°46'26.40"W	2288
	<b>Ask6</b>	granite	30°52'40.80"N 7°46'15.60"W	2362
	<b>Ask5</b>	granite	30°49'51.60"N 7°47'9.60"W	2085
	<b>04Si</b>	granite	30°48'51.35"N 7°34'51.25"W	2150
	<b>03Si</b>	granite	30°47'32.57"N 7°43'46.16"W	2130
	<b>Ask4</b>	granite	30°46'40.80"N 7°46'55.20"W	1917
	<b>Ask3</b>	granite	30°43'37.20"N	1940

			7°46'19.20"W	
	<b>SI0401</b>	granite	30°43'30.00"N	1931
			7°46'16.00"W	
<i>Southern Foreland Block SF3</i>	<b>SI0402</b>	granite	30°41'4.00"N	1965
			7°46'21.00"W	
	<b>Ask2</b>	granite	30°38'42.00"N	1907
			7°48'7.20"W	
	<b>SI0403</b>	granite	30°37'6.00"N	1822
			7°49'39.00"W	
	<b>SI0404</b>	matr. congl.	30°35'51.00"N	1355
			7°50'39.00"W	
		pebble		
	<b>SI0405</b>	congl.	30°35'51.00"N	1355
			7°50'39.00"W	
<b>Western MHA</b>				
<i>Block WB1</i>	<b>BO01</b>	granite	31°14'57.33"N	860
			8°30'11.59"W	
	<b>AZ03</b>	granite	31°10'59.34"N	1820
			8°20'18.99"W	
	<b>AZ04</b>	granite	31°10'59.34"N	1820
			8°20'18.99"W	
	<b>AZ01</b>	granite	31° 9'11.59"N	1480
			8°18'19.92"W	
	<b>AZ02</b>	granite	31° 9'11.59"N	1480
			8°18'19.92"W	
<i>Block WB2</i>	<b>ALM01</b>	granite	31° 6'50.07"N	1950



		8°22'51.06"W	
<b>ALM02</b>	granite	31° 6'35.33"N	1950
		8°23'5.59"W	
<b>AD01</b>	granite	31° 6'45.66"N	1135
		8°30'38.23"W	

**Table S2.** Results of the different tests led for thermal modeling of AZ01-02 and AZ03-04 samples.

<u>Tests for AZ01-02</u>		<i>HT1 pred</i>	<i>HT1 SP</i>	<i>HT2 pred</i>	<i>HT2 SP</i>	<i>HT3 pred</i>	<i>HT3 SP</i>
<i>eU</i>	<i>obs data</i>	AZ01-02	AZ01-02	AZ01-02	AZ01-02	AZ01-02	AZ01-02
14.7	65	55	40	54	40	51	40
14.1	14	34	20	33	20	27	20
27.8	33	68	58	68	58	71	57
18.8	30	39	25	39	25	35	26
30.5	48	38	29	38	29	37	29
13.5	68	25	14	25	15	19	14
16.5	64	27	15	27	15	21	15
37.5	56	54	45	53	45	56	45
28.6	89	70	59	69	59	72	58
140.2	103	134	103	120	102	143	101
27.2	49	52	41	51	41	52	41
41.1	47	54	46	54	46	57	45
<i>AFT</i>	136	132	111	130	112	130	115
<i>MTL</i>	11.2	10.7	10.7	11	10.9	10.6	10.6
<i>Dpar</i>	1.72	2.04	2.04	2.0	2.0	2.0	2.0
<i>LL</i>		-1013		-984		-872	

<u>Tests for AZ03-04</u>		<i>HT1 pred</i>	<i>HT1 SP</i>	<i>HT2 pred</i>	<i>HT2 SP</i>	<i>HT3 pred</i>	<i>HT3 SP</i>
<i>eU</i>	<i>obs data</i>	AZ03-04	AZ03-04	AZ03-04	AZ03-04	AZ03-04	AZ03-04
30.6	77	61	54	60	54	66	54
20.9	60	55	46	54	46	59	47
38.7	79	84	69	84	68	92	69
31.1	94	71	63	70	63	78	63
32.8	35	59	52	58	52	64	52
27.7	86	70	63	70	63	77	63
43.4	104	109	77	106	76	120	77
39.7	61	118	81	113	81	128	81
<i>AFT</i>	130	132	108	129	108	131	112
<i>MTL</i>	11.7	10.8	11	11.1	11.1	10.8	11
<i>Dpar</i>	1.68	1.84	1.84	1.8	1.8	1.7	1.7
<i>LL</i>		-560		-527		-667	

**Table S3.** Results of forward modeling for AD01 sample.

	<i>obs data</i>	Forward modeling						
		<i>predicted data</i>						
		<i>HT1f</i>	<i>HT2f</i>	<i>HT3f</i>	<i>HT5f</i>	<i>HT6f</i>	<i>HT7f</i>	<i>HT8f</i>
<b>Uncorrected AHe ages</b>	6	6	6	7	7	7	7	7
	4	7	7	14	11	11	8	8
	5	6	7	13	11	11	7	8
	10	11	12	21	17	16	12	12
	15	12	13	22	18	18	14	13
	4	5	5	5	6	5	6	6
	6	5	5	5	6	6	6	6
<b>LogLikelihood</b>		<b>-569</b>	<b>-588</b>	<b>-2064</b>	<b>-1283</b>	<b>-1231</b>	<b>-645</b>	<b>-724</b>